



Università degli Studi di Bari Aldo Moro

Dipartimento Interateneo di Fisica

Dottorato In Fisica XXXI Ciclo

Search for resonances decaying into muon pairs with the CMS experiment at LHC

Relazione di fine Terzo Anno

Tutor:
Dott.ssa Anna Colaleo

Dottorando:
Filippo Errico

Chapter 1

Search for resonances decaying into muon pairs with the CMS experiment at LHC

My PhD activity deals with the search for resonances decaying into muon pairs with the CMS detector [1] at LHC.

Muons play a central role in CMS being the most natural and powerful tool to detect interesting events over the background. They are:

- less affected than electrons by radiative losses in the tracker material
- stand out after the high magnetic field
- stand out from the large hadronic background typical of hadron colliders

CMS has a dedicated system to detect muons (the so call muons system) composed of different detectors which allows to measure muon momentum with a resolution less then 20% for muons with momentum of the order of TeV [2].

In particular I am focusing on the search, at low mass, for the Standard Model Higgs and, at high mass, for new narrow resonances (with a mass of the order of TeV) predicted in several models Beyond Standard Model, decaying into muons.

1.1 Search for the Standard Model Higgs

I am involved in the search for Standard Model Higgs produced via Vector Boson Fusion (VBF) and decaying into two muons. Even if VBF has the second largest cross section (the first is the gluon-gluon fusion production), it has a bigger sensitivity thanks to its powerful discrimination against background: this mechanism proceeds by the scattering of two (anti-)quarks, mediated by exchange of a W or Z boson, with the Higgs boson radiated off the weak-boson propagator. The scattered quarks give rise to two hard jets in

the forward and backward regions of the detector. Gluon radiation in the central-rapidity is suppressed thanks to the color-singlet nature of the weak-gauge boson exchanged: this feature allows to distinguish VBF from overwhelming QCD backgrounds including gluon-fusion induced Higgs + 2 jets production and production of H in association with a W or Z boson hadronically decaying. At the same time, thanks to the excellent muon momentum resolution at CMS, most $H \rightarrow \mu\mu$ events can be measured with an invariant dimuon mass resolution of 1.5 to 2.5 GeV, despite Higgs natural width (~ 4 MeV). This allows me to discriminate the expected signal events against the vast quantities of high-mass, off-shell $Z \rightarrow \mu^+\mu^-$ decays, as well as leptonic $t\bar{t}$ decays, which form the main backgrounds.

This analysis is most important because $H \rightarrow \mu\mu$ cross section measurement allows to measure different Higgs boson properties, such as the Higgs-muon Yukawa coupling strength, and compare it to the muon mass; at the same time measure the ratio of the $H \rightarrow \mu\mu$ to $H \rightarrow \tau\tau$ cross sections can provide constraints on the proportionality of the Higgs couplings to fermions of different generations, and of leptons with different masses.

The best results to date on Higgs coupling to second fermion generation, with 2016 data, are $2.64 \times$ SM prediction for 13 TeV for the observed upper limit on the rate of production of a Higgs boson with the mass of $125 \text{ GeV}/c^2$ (σ/σ_{SM}) and an observed significance of 0.9 standard deviations [3]. In order to improve these results, obtained with cut flow selection, I have performed the analysis with the multivariate analysis approach. The idea is to separate VBF decay channel, using appropriate cuts, from the inclusive decay and then, on this signal region, create a variable, starting from the usual ones (e.g. mass, momentum, angular variables), in order to be able to separate signal and background as much as possible; this distribution will be then used for limit extraction.

Figure 1.1 shows the variable distribution obtained combining different variables (some of them are plotted in Figure 1.2) with a binary tree (BDTG) and neural network (MLP).

I have started to analyse 2016 data, corresponding to 35.9 fb^{-1} , in order to compare this strategy with one used to produce latest results and then move to 2017 and 2018 data.

With this approach, I obtain the best results using the neural network (MLP):

- $2.35 \times$ SM prediction for expected upper limit on the rate of production of the Higgs boson
- 0.942 (0.993 - stat. only) standard deviations

Looking at these values, it seems this strategy could help in improving published results.

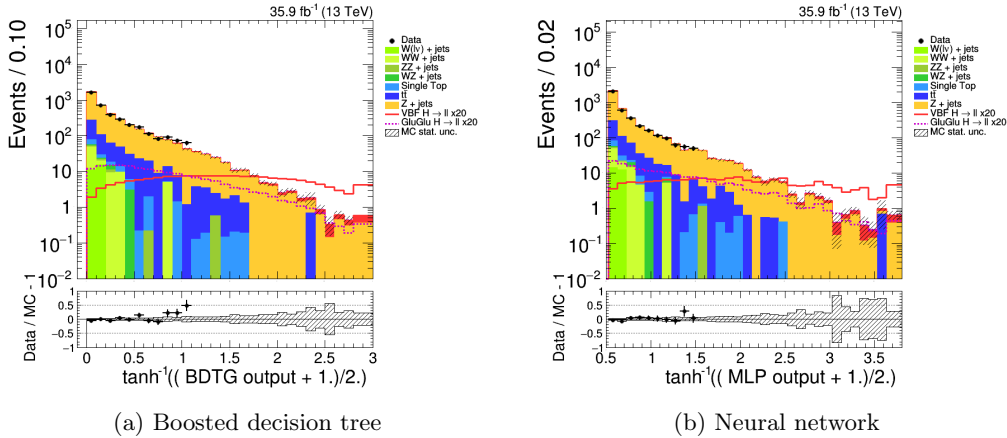


Figure 1.1: Multivariate analysis: validation plot for two different approach, BDTG (left) and MLP (right).

1.2 Search for new massive resonances

The current Particle Physics is well described by the Standard Model (SM) even if there are some aspects SM is not able to take into account (e.g. dark matter, gravitational force). In order to try to solve these issues, many models have been developed beyond Standard Model (BSM) and within these, new bosons, like Z' , are introduced: examples include models described with extended gauge groups, featuring additional U(1) symmetries such as the Sequential Standard Model (SSM) [4] that includes a Z'_{SSM} boson with SM-like couplings, the Grand Unification Theories (GUT) inspired SSM models, based on E6 gauge group, with a Z'_ψ boson and the Kaluza - Klein graviton (GKK) of the Randall - Sundrum (RS) model of the Extra Dimensions [5]. The results of the analysis performed searching for a new massive resonance can be also reinterpreted in the context of simplified models of Dark Matter (DM) particles that obtain sizeable interactions with fermions through an additional spin-1 high-mass particle mediating the SM-DM interaction [6].

1.2.1 p_T assignment

Muons involved in this analysis have p_T of the order of TeV, the so called “high- p_T ” muons and, due to the high energy, the probability for the muons to produce electromagnetic showers increases; such showers can corrupt the measurement done in the muon detectors. Therefore, a set of specially-developed TeV-muon track fits has been developed to carefully treat the information from the muon system. The “tracker-plus-first-muon-station” (TPFMS) fit only uses hits from the tracker and the innermost muon station with hits; this is in order to be insensitive to the stations that are farther along the muon’s trajectory and thus possibly contaminated by showers, due to the larger

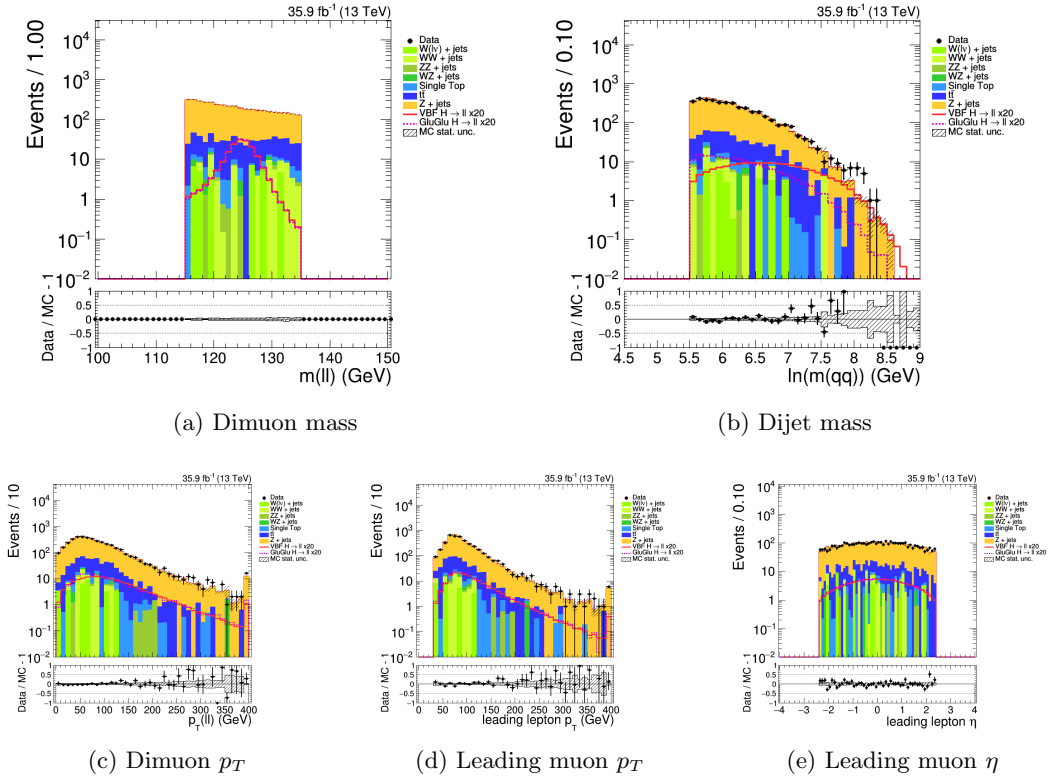


Figure 1.2: Validation plots for different variables used to train multivariate analysis: dimuon and dijet mass on top, dimuon p_T , p_T and η of the leading muon on bottom.

amount of iron traversed by the muon. The “Picky” fit uses all tracker hits, while a selection is applied to muon hits. The hits from stations with a high probability of shower contamination (determined from the hit occupancy) are required to have a χ^2 with respect to the trajectory below a certain threshold. The “dynamic truncation” (DYT) fit takes into account possible energy losses from radiative processes and tries to avoid hits produced after a large energy loss in the muon system. For every silicon tracker track identified as belonging to a muon by the global fit, the result of the tracker-only fit is propagated out to the muon stations and attempts are made to add compatible muon hits to the fit. For each hit the compatibility between the extrapolated tracker track and the reconstructed segment in the muon chambers is calculated, using an estimator that in absence of correlation reduces to a χ^2 . Momentum assignment is finally performed by the “Tune P” algorithm, which chooses the best muon reconstruction between global-track, tracker-track, TPFMS, Picky, and DYT. The selection is made on a track-by-track basis, using the track fit χ^2/ndf tail probability and the relative p_T measurement error σ_{p_T}/p_T .

I have performed studies on TuneP assignment using simulation (2016) and 2016 and

2017 data, in different p_T ranges and in two mass regions. Figure 1.3 shows an example of p_T distribution, after TuneP assignment together with p_T distribution reconstructed with Picky and Dyt algorithm comparing simulation and 2016 plus 2017 data.

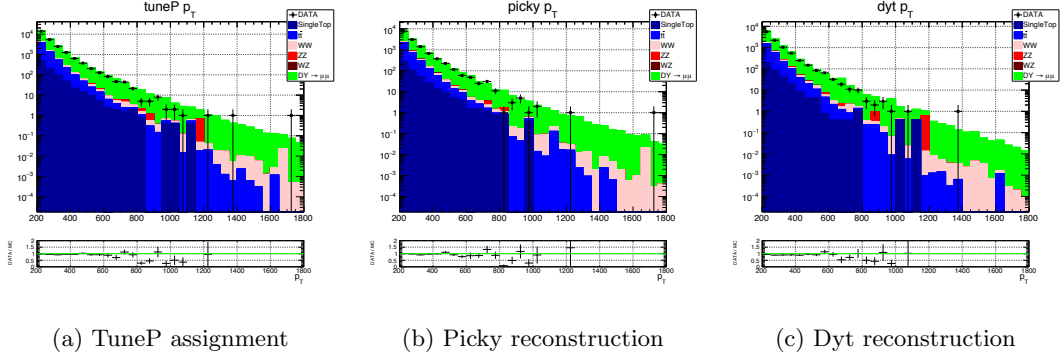


Figure 1.3: p_T distribution: TuneP on the left, Picky in the middle and Dyt on the right. Stack plot is the simulation; data (2016 plus 2017) are the black dots. In the bottom panel, data/MC ratio is reported.

1.2.2 Mass distribution

I am focusing on the search for new massive boson decaying into two muons: this channel benefits from high signal selection efficiencies and relatively small, well-understood, backgrounds. The dominant and irreducible SM background arises from Drell-Yan (DY) production (Z/γ^*) of $\mu^+\mu^-$ pairs. Additional sources of background are top - antitop quark ($t\bar{t}$) and single top quark (tW), Drell-Yan $\tau^+\tau^-$ and diboson (WW, ZZ, WZ), in which the two prompt leptons are from different particles. These processes are estimated using Monte Carlo (MC) simulated events at the next-to-leading order (NLO) and corrected to the next-to-next-to-leading order (NNLO). Events in which at least one lepton candidate is a misidentified jet (W+jets, γ +jets and multijets) contribute a small background in the mass region of interest. These contributions are estimated from data.

I have analyzed 2017 data, corresponding to $41.9 fb^{-1}$; in Figure 1.4, the comparison between data and Monte Carlo of the dilepton mass distribution is shown without evidence for a signal deviation from the SM expectations.

In order to handle properly the different muon momentum resolution between barrel and endcaps, the scale bias and any source of inefficiency, the analysis is performed in two pseudorapidity categories: barrel-barrel (BB) events, in which both muons are in the barrel and events with at least one of the two muons is in the endcaps (BE). The corresponding mass distributions are shown in Figure 1.5

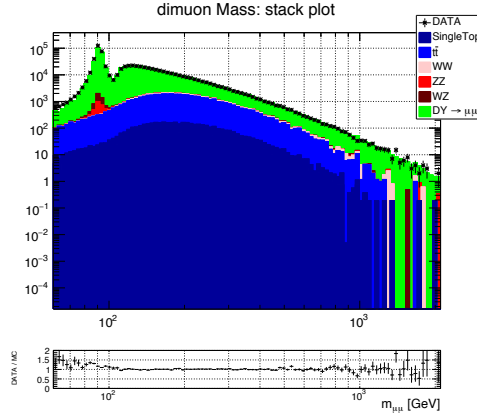


Figure 1.4: The invariant mass spectrum, together with the predicted SM backgrounds. In the bottom panel, data/MC ratio is reported. No evidence for a signal deviation from the SM expectations is observed.

1.2.3 Dimuon mass resolution

I have evaluated mass experimental resolution from DY simulation as a function of the generated dimuon mass in different η categories. For each considered mass bin, the residual has been measured comparing the reconstructed mass with the generated one: each residual is then fit using Cruijff function, the experimental function describing the resolution. This function is the convolution of a Breit–Wigner (BW) function, describing the intrinsic signal shape, and a Gaussian with asymmetric exponential. The resolution is finally defined as the σ of the aforementioned function: Figure 1.6 shows dimuon mass resolution for different mass ranges and different η categories. Comparing 2017 results with 2016, an improvement of about 20% for mass of 4 TeV is visible mainly due to new alignment scenario.

1.2.4 Mass scale

The response of the detector to the dilepton mass may evolve as the mass increases: as the muon p_T increases, it becomes more and more sensitive to the detector alignment and to the magnetic field. To estimate these effects of the p_T to the dimuon mass, I have recomputed the Drell-Yan mass in simulation by applying a shift (a bias) to the muon p_T . The shift is applied to each muon and as a function of η and ϕ . The values of the bias have been calculated by matching the distribution charge/ p_T in simulation and data.

The correction has been performed only for the BE+EE category, given the p_T bias consistent with zero in the barrel. Figure 1.7 shows the dimuon mass resolution obtained with and without the correction, for the BE category. The observed difference is greater

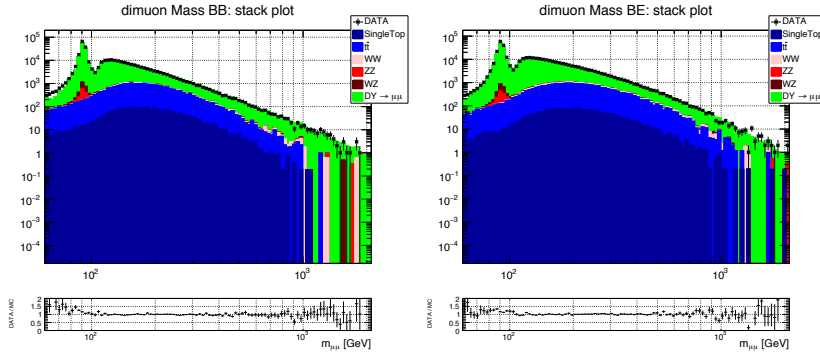


Figure 1.5: The invariant mass spectrum, together with the predicted SM backgrounds: on the left in BB category and on the right in BE. In the bottom panel, data/MC ratio is reported. No evidence for a signal deviation from the SM expectations is observed.

then 40% at 5 TeV.

To estimate also the effect of the measured p_T bias to the dimuon mass reconstructed with data, I have recomputed the mass by applying a shift to the muon p_T . Again, the correction has been performed only for the BE events. For different mass ranges, the relative residuals have been plotted comparing the reconstructed mass with the value obtained correcting the muon p_T in data: $(\text{mass} - \text{mass}_{\text{corrected}})/\text{mass}$. Figure 1.8 shows the mean value of such distributions as a function of the mass. No shift is observed in the mass value corrected by the p_T bias.

1.2.5 MC distribution mass fit

In order to test for the existence of a resonance, a shape analysis has been performed using an unbinned maximum likelihood fit of dimuon invariant mass values m (the observable) to search for a resonant peak on-top of the smooth background distribution. Data is fit with a sum of signal and background shapes: while signal has been parametrized by the convolution of a Breit-Wigner (describing the intrinsic signal shape) and a Gaussian distribution (describing the experimental resolution), background parametrization has been obtained by fitting the SM simulated background distribution. I have fit the distribution mass in order to obtain the probability density function used to extract limit, in the mass range [150, 5000] GeV. In Figure 1.9, the fit of the MC mass distributions are shown for Barrel - Barrel and Barrel - Endcap & Endcap - Endcap Region.

The final limit, set on the parameter R_σ which is the ratio of the cross section for dilepton production through a Z' boson to the cross section for dilepton production through a Z boson, are shown in Figure 1.10.

For the Z'_{SSM} particle and for the superstring inspired Z'_ψ particle, the new 95% confidence level lower mass limits are found to be 4.35 TeV and 3.95 TeV, with respect to the old one, 4.30 TeV and 3.75 TeV respectively [7].

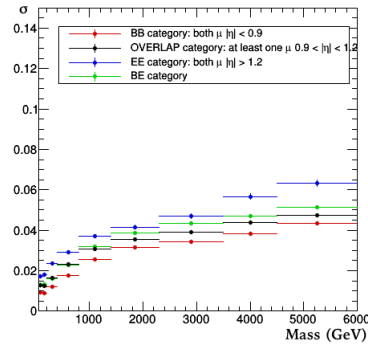


Figure 1.6: Dimuon mass resolution as a function of dimuon mass evaluated in different η ranges.

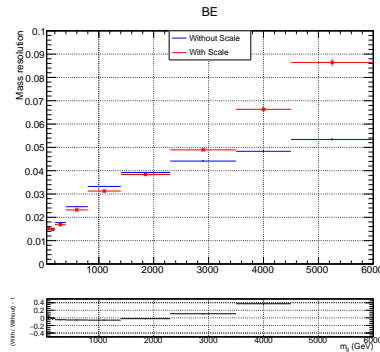


Figure 1.7: Dimuon mass resolution as a function of dimuon mass evaluated in the BE category with (in red) and without (in blue) the p_T scale propagated, for DY simulated events.

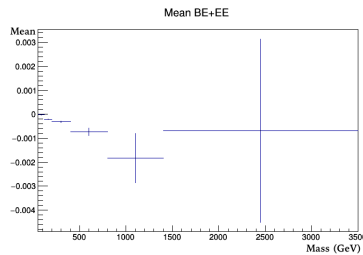


Figure 1.8: Mean value, as a function of the mass, of the relative mass residuals estimated comparing the reconstructed mass with and without the p_T bias correction in data.

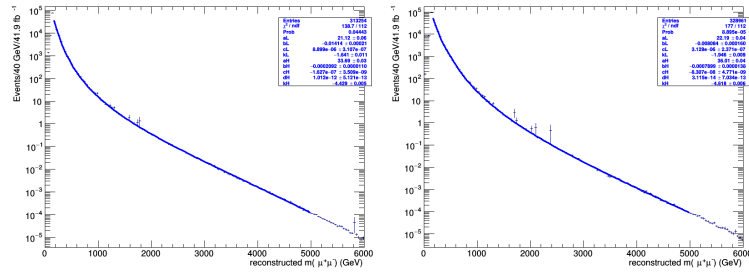


Figure 1.9: Fit of the simulated mass distribution: on the left for BB category; on the right for BE.

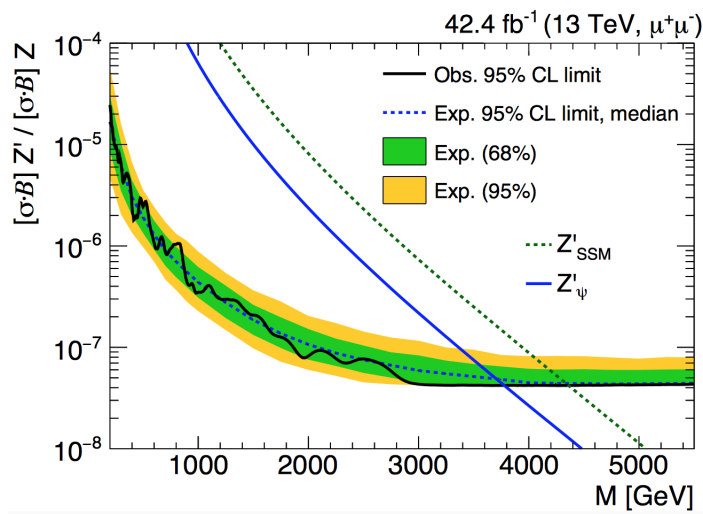


Figure 1.10: Final limits for Spin 1 resonance.

Chapter 2

School & conferences

2.1 School

- ESHEP: European Schools of High-Energy Physics, 20 June - 3 July, Maratea, Italy
<https://physicschool.web.cern.ch/physicschool/ESHEP/default.html>

2.2 Conferences

- Les Rencontres de Physique de la Vallée d'Aoste, 26 February - 03 March 2018, La Thuile (Italy). <https://agenda.infn.it/conferenceDisplay.py?confId=14377>
Proceeding: “*Search for high-mass resonances in the dilepton final state in p-p collisions at $\sqrt{s}=13$ TeV*”

Bibliography

- [1] CMS Collaboration, “The CMS experiment at the CERN LHC”, JINST 3:S08004,2008
- [2] CMS Collaboration, “Performance of muon reconstruction including Alignment Position Errors for 2016 Collision Data”, CMS DP-2016/067
- [3] CMS Collaboration, “Search for the Higgs boson decaying to two muons in proton-proton collisions at $\sqrt{s}= 13$ TeV”, arXiv:1807.06325 [hep-ex]
- [4] A. Leike, “The Phenomenology of Extra Neutral Gauge Bosons”, Phys. Rept. 317 (1999) 143, [hep-ph/9805494]
- [5] L. Randall, R. Sundrum, “A Large Mass Hierarchy from a Small Extra Dimension”, Phys. Rev. Lett. 83 (1999) 3370, [hep-ph/9905221]
- [6] A. Albert et al., “Recommendations of the LHC Dark Matter Working Group: Comparing LHC searches for heavy mediators of dark matter production in visible and invisible decay channels”, (2017). arXiv:1703.05703.
- [7] CMS Collaboration, “*Search for high-mass resonances in dilepton final states in proton-proton collisions at $\sqrt{s} = 13$ TeV*”, JHEP 1806 (2018) 120, 10.1007/JHEP06(2018)120